



**HAL**  
open science

## High-pass NGD characterization of resistive-inductive network based low-frequency circuit

Fayu Wan, Xiaoyu Huang, Konstantin Gorshkov, Bogdana Tishchuk, Xiaofeng Hu, George Chan, Frank Elliot Sahoo, Sahbi Baccar, Mathieu Guerin, Wenceslas Rahajandraibe, et al.

### ► To cite this version:

Fayu Wan, Xiaoyu Huang, Konstantin Gorshkov, Bogdana Tishchuk, Xiaofeng Hu, et al.. High-pass NGD characterization of resistive-inductive network based low-frequency circuit. *COMPEL: The International Journal for Computation and Mathematics in Electrical and Electronic Engineering*, 2021, 40 (5), pp.1032-1049. 10.1108/COMPEL-05-2021-0160 . hal-03605224

**HAL Id: hal-03605224**

**<https://hal.science/hal-03605224>**

Submitted on 10 Mar 2022

**HAL** is a multi-disciplinary open access archive for the deposit and dissemination of scientific research documents, whether they are published or not. The documents may come from teaching and research institutions in France or abroad, or from public or private research centers.

L'archive ouverte pluridisciplinaire **HAL**, est destinée au dépôt et à la diffusion de documents scientifiques de niveau recherche, publiés ou non, émanant des établissements d'enseignement et de recherche français ou étrangers, des laboratoires publics ou privés.

# High-pass NGD resistive-inductive network based low-frequency circuit characterization

Fayu Wan<sup>1</sup>, Xiaoyu Huang<sup>1</sup>, Konstantin Gorshkov<sup>2</sup>, Bogdana Tishchuk<sup>2</sup>, Xiaofeng Hu<sup>3</sup>, George Chan<sup>4</sup>, Frank Elliot Sahoo<sup>5</sup>, Sahbi Baccar<sup>6</sup>, Mathieu Guerin<sup>7</sup>, Wenceslas Rahajandraibe<sup>7</sup> and Blaise Ravelo<sup>1</sup>

<sup>1</sup> Nanjing University of Information Science & Technology (NUIST), Nanjing, China

<sup>2</sup> ITMO University, Saint Petersburg, Russia

<sup>3</sup> Army Engineering University of PLA, National Key Laboratory of Electromagnetic Environment Effect, Shijiazhuang, China

<sup>4</sup> ASM Pacific Technology Ltd., Hong-Kong

<sup>5</sup> Laboratoire de Physique Nucléaire et Physique de l'Environnement (LPNPE), Univ. d'Antananarivo - Madagascar

<sup>6</sup> CESI Ecole d'Ingénieurs, Rouen, France

<sup>7</sup> Aix-Marseille University, CNRS, University of Toulon, IM2NP UMR7334, Marseille, France

Email: fayu.wan@nuist.edu.cn, 1724948024@qq.com, k.gorshkov@list.ru, b.tishchuk@list.ru, george.chan@asmpt.com, snowfox2270@163.com, sbaccar@cesi.fr, mathieu.guerin@im2np.fr, wenceslas.rahajandraibe@im2np.fr, blaise.ravelo@yahoo.fr

Corresponding author: snowfox2270@163.com

**Abstract:** Recent studies reveal the design feasibility of negative group delay (NGD) electronic circuits. There are different classes of NGD electronic circuits. However, so far, few research works are available on the design method of typical high-pass (HP) NGD circuits. The present paper investigates on the theory, design and test of an unfamiliar HP-NGD circuit. The HP-NGD passive topology is constituted by resistive-inductive (RL) parallel network. The main specifications of the HP-NGD function are defined. Then, the analytical theory from the voltage transfer function examination is established. The synthesis equation of the HP-NGD circuit parameters in function of the ideal specifications are elaborated. Then, two different prototypes of RL HP-NGD circuit implemented on printed circuit board constituted by discrete components are designed and fabricated. An innovative measurement technique of the HP NGD circuit is developed based on the sine frequency tuning. As expected, calculated, simulated and measured results are in good correlation. HP-NGD responses with NGD optimal frequency, value and attenuation of about (9 MHz, -1.12  $\mu$ s, -1.64 dB) and (21 MHz, -0.92  $\mu$ s, -4.81 dB) are measured. The tested circuits have experimented NGD cut-off frequencies around 5 MHz and 11.7 MHz, respectively.

**Keywords:** High-pass (HP) negative group delay (NGD), RL-network, circuit theory, NGD measurement technique.

## 1/ INTRODUCTION

Most of communication devices are regularly victim of undesirable delay effects [1-2]. There are different sources of delays at different level of communication systems. For example, at electronic component levels the interconnect complexity induces signal delays and distortions [3-4] Because of such imperfection, the leading and tailing edges of pulse communication signals can be significantly distorted [5-6]. Against the delay, an innovative synthesis of delay-insensitive circuits was introduced [7]. For some cases of communication systems, the delay effects are exploited to identify the communication channel [8], to design recirculating delay line [9], to design a transmission line (TL) delay-based RFID tag [10] and also to improve the gain-bandwidth product of amplifiers [11].

An orthodox technique of delay equalization, which is less familiar to most electronic engineers, based on the use of negative group delay (NGD) function was also introduced for the interconnect effect [12], the filter phase linearization [13] and unconditional stable active filter [14]. However, compared to the other electronic functions (filter, amplifier, antenna, oscillator, power combiner/divider, ...), the unfamiliar NGD ones are less familiar to most electronic design engineers. For this reason, the present study introduces a further investigation on typical high-pass (HP) NGD circuit by using resistive-inductive (RL) passive network. Before the exploration of the HP-NGD developed study, we propose to start with the state art.

The NGD function was initially experimented with negative group velocity (NGV) medium at optical wavelengths [15-20]. The NGD effect was investigated as abnormal and superluminal phenomena [17,19-20]. Then, the NGD research topic attracted some of electronic and RF and microwave engineering researchers [21-31]. Design and test of microwave NGD circuits with metamaterial negative refractive index (NRI) structures were performed [21-24]. Based on the analogy between the transfer function of 3-D and 2-D structures and 1-D microstrip circuits, topologies of RLC-resonant cells analog to the split ring resonator cell were identified [24-25]. In parallel to the development of microwave circuit design, innovative topologies of low-frequency NGD circuit using R, L, C and operational amplifier components were proposed [26-30]. Different simulations and experimental demonstrations of NGD effect [28-31] were successfully realized. Thus, despite the implicit counterintuitive effect, it was emphasized that the NGD function does not contradict the causality [26-27]. Last two decades, different design of active circuits based on bilateral gain-compensated [32], current-feedback operational-amplifier and uses grounded resistors and capacitors [33], and broadband switch-less bi-directional amplifier [34] circuits were proposed.

Despite the proposed various circuits, the meaning of the NGD function remains an open question. For the better understanding, the NGD theory based on the similitude between the filter behavior [35-36] was initiated. The concept of low-pass (LP) [37] and high-pass (HP) [38] NGD functions was initiated. But so far, few research works are available in the literature on the HP-NGD topology. For this reason, the present paper is focused on the investigation on the HP-NGD topology using RL-network.

The paper is organized in three main sections:

- Section 2 defines analytically the main specifications of the HP-NGD ideal responses by considering illustrative representative GD and magnitude diagrams. Then, the voltage transfer function (VTF) of the RL-network based passive circuit is formulated.

- By examining the VTF, Section 3 develops the theorization of the RL-network based HP-NGD passive circuit. The synthesis method allowing to determine the RL-circuit resistor and inductor parameters is elaborated in function of the desired HP-NGD specifications.
- Section 4 describes the prototypes of the fabricated HP-NGD passive circuits as a proof-of-concept (POC) are described. Then, the experimental setup of the HP-NGD prototype is introduced.
- Section 5 examines the experimental validation results. The comparisons of calculated, simulated and measured results will be discussed.
- Section 6 is the final conclusion.

## 2/ HIGH-PASS (HP) NGD THEORETICAL SPECIFICATIONS

The present section elaborates the theoretical approach of HP-NGD circuit. After the ideal specifications, the analytical formulations of the NGD existence condition in function of the constituting RL-network parameters will be developed.

### 2-1/ Basic analytical parameters

The proposed NGD circuit is based on the diagram shown by Fig. 1. It is constituted by two-port with input voltage  $V_{in}$  and output voltage  $V_{out}$ . The NGD analysis is based on the GD response from the voltage transfer function (VTF).



**Fig. 1: NGD circuit black box diagram.**

According to the circuit and system theory, the VTF is traditionally defined by:

$$N(s) = \frac{V_{out}(s)}{V_{in}(s)} \quad (1)$$

with  $s=j\omega$  is the Laplace variable. By definition, the corresponding transmittance isochrone is written as:

$$N(j\omega) = \Re[N(j\omega)] + j\Im[N(j\omega)] \quad (2)$$

with  $\Re(z)$  and  $\Im(z)$  are real and imaginary parts. By definition, the associated magnitude is given by:

$$N(\omega) = |N(j\omega)| = \sqrt{\Re[N(j\omega)]^2 + \Im[N(j\omega)]^2} . \quad (3)$$

The associated phase is expressed by:

$$\varphi(\omega) = \arg[N(j\omega)] = \arctan \left[ \frac{\Im[N(j\omega)]}{\Re[N(j\omega)]} \right]. \quad (4)$$

The GD derived analytically from this transmission phase is defined by:

$$GD(\omega) = \frac{-\partial\varphi(\omega)}{\partial\omega}. \quad (5)$$

Knowing these basic parameters, the specifications of the HP-NGD response are defined in the following subsection.

### 2-2/ Definition of HP-NGD response

An electronic circuit can be assumed as a HP-NGD function if the GD at very low-frequencies (VLFs), defined by  $\omega \approx 0$ , satisfies the condition:

$$GD(\omega \approx 0) > 0. \quad (6)$$

The associated cut-off angular frequency,  $\omega_n$ , is the root of equation:

$$GD(\omega_n) = 0. \quad (7)$$

This means that we should satisfy the inequality conditions:

$$\begin{cases} GD(\omega \leq \omega_n) > 0 \\ GD(\omega > \omega_n) \leq 0 \end{cases} \quad (8)$$

as explained by the ideal diagram of Fig. 2(a). In addition to the GD response, the VTF magnitude response as shown in Fig. 2(b) must be specified.

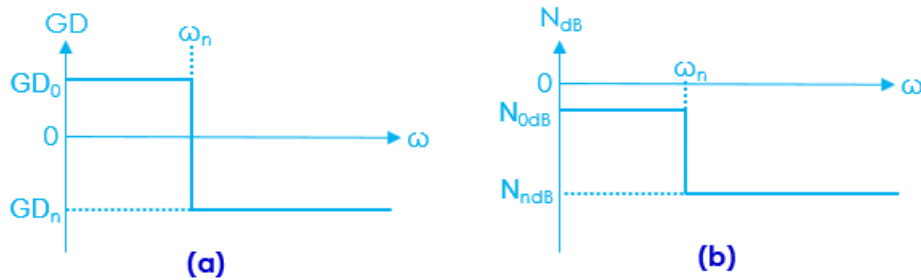


**Fig. 2: Ideal responses of VTF (a) GD and (b) magnitude.**

For example, the LP-NGD circuit can be designed by expecting a desired attenuation:

$$N(\omega \approx 0) = N_0 < 1. \quad (9)$$

As materialization of this ideal specification, a topology of RL-network based circuit will be analyzed in the following subsection.

### 2-3/ HP-NGD analysis

The present HP-NGD analysis is theoretically inspired from the LP-NGD one [35-38] from the VTF exploration. Fig. 3 introduces the RL-network based passive circuit under investigation. This passive topology is composed by a series  $R_m$  resistor shunted by series RL-network. It can be demonstrated from voltage divider principle that the VTF model of the considered RL-circuit is given by:

$$N(s) = \frac{R_m(R + Ls)}{RLs + R_m(R + Ls)}. \quad (10)$$

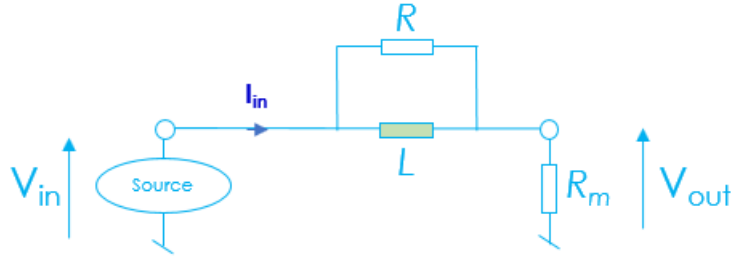


**Fig. 3: Topology of HP-NGD passive circuit.**

The previous equation implies the transmittance isochrone as a complex number expressed as:

$$N(j\omega) = \frac{R_m(R + jL\omega)}{R_mR + jL\omega(R + R_m)}. \quad (11)$$

The magnitude corresponding to this VTF transmittance can be written by:

$$N(\omega) = |N(j\omega)| = \frac{R_m\sqrt{R^2 + (L\omega)^2}}{\sqrt{(R_mR)^2 + (L\omega)^2(R + R_m)^2}}. \quad (12)$$

Based on equation (3), the associated phase is given by:

$$\varphi(\omega) = \arctan\left(\frac{L\omega}{R}\right) - \arctan\left[\frac{L\omega(R + R_m)}{R_mR}\right]. \quad (13)$$

The GD is calculated from this equation by means of the mathematical definition of relation (4):

$$GD(\omega) = \frac{LR^2[R^2R_m - L^2\omega^2(R + R_m)]}{(R^2 + L^2\omega^2)[R^2R_m + L^2\omega^2(R + R_m)^2]}. \quad (14)$$

Knowing these fundamental expressions, we can make the NGD analysis by considering the particular frequencies as reported in the following section.

### 3/ HP-NGD ANALYSIS AND SYNTHESIS METHOD

The existence condition of HP-NGD behavior can be generally demonstrated by the calculation of the GD established previously at different particular frequencies. The following paragraphs examines the analytical investigation at very low frequencies (VLFs) and the NGD cut-off frequency.

#### 3-1/ VLF analysis of the RL-network based topology

The most intuitive analysis of the RL-network topology understudy can be performed at VLF where \$\omega \approx 0\$. Accordingly, the VTF magnitude expressed in equation (12) is transformed as:

$$N_0 = N(\omega = 0) = \frac{R_m}{R_m + R}. \quad (15)$$

Always at VLF ( $\omega \approx 0$ ), the GD given by equation (14) becomes:

$$GD_0 = GD(\omega \approx 0) = \frac{L}{R_m}. \quad (16)$$

We can see that this GD is always positive,  $GD_0 > 0$ . This analytical finding explains the necessary condition of the HP-NGD. The next step of the demonstration must be the existence of the NGD cut-off frequency.

### 3-2/ Analysis at NGD cut-off frequency

The NGD cut-off frequency is the solution of equation (7) by considering the GD formulated in equation (14). Accordingly, we have the quantity versus the RL-network parameters:

$$\omega_n = \frac{R\sqrt{R_m}}{L\sqrt{R_m + R}}. \quad (17)$$

Substituting this cut-off frequency into the attenuation established in equation (12), we have:

$$N(\omega_n) = \frac{\sqrt{R_m}}{\sqrt{R_m + R}}. \quad (18)$$

For the positive real coefficient,  $x > 1$ , we can demonstrate that the GD at the multiple of angular frequency,  $x\omega_n$ , is equal to:

$$GD(x\omega_n) = \frac{(1-x^2)L(R+R_m)}{[R+(1+x^2)R_m][x^2R+(1+x^2)R_m]}. \quad (19)$$

Under the hypothesis  $x > 1$ , it can be understood from this expression that this GD is always negative:

$$GD(x\omega_n) < 0. \quad (20)$$

Moreover, the attenuation of the VTF magnitude written in equation (12) at this angular frequency,  $x\omega_n$ , is formulated by:

$$N(x\omega_n) = \frac{\sqrt{R_m[R+(1+x^2)R_m]}}{\sqrt{(R+R_m)[x^2R+(1+x^2)R_m]}}. \quad (21)$$

Knowing the positive GD established by equation (16) and the existence of the cut-off frequency given by equation (17), this analytical result illustrates the HP-NGD behavior of the RL-network topology introduced by Fig. 3.

### 3-3/ NGD optimal frequency

In opposite to the case of LP-NGD function investigated in [37], the HP-NGD circuit should present an optimal angular frequency,  $\omega_x$ , where:

$$GD(\omega_x) = \min[GD(\omega)]. \quad (22)$$

This NGD optimal frequency should verify the relation:

$$\left. \frac{\partial GD(\omega)}{\partial \omega} \right|_{\omega=\omega_x} = 0. \quad (23)$$

After resolution of this equation, we can demonstrate that the following optimal frequency written as:

$$\omega_x = \frac{R\sqrt{R_m \left[ (R + 2R_m)(R_m + R) + \sqrt{R_m(R + R_m)^3} \right]}}{L(R_m + R)}. \quad (24)$$

For the sake of mathematical simplification, we can assume that this optimal angular frequency in function of NGD cut-off frequency, for example, by taking:

$$\omega_x = x\omega_n. \quad (25)$$

In other words, by means of equation (17) and equation (24) of characteristic angular frequencies, the real coefficient can be expressed in function of the HP-NGD circuit resistive parameters as:

$$x = \frac{\omega_x}{\omega_n} = \frac{\sqrt{\left[ (R + 2R_m)(R_m + R) + \sqrt{R_m(R + R_m)^3} \right]}}{\sqrt{R_m + R}}. \quad (26)$$

The optimal GD written in relation (4) can be determined by choosing:

$$GD(\omega_x) = GD(x\omega_n) < 0. \quad (27)$$

Under the same approach, the attenuation of the RL-network topology at the optimal angular frequency can be formulated as:

$$N(\omega_x) = N(x\omega_n) < 1. \quad (28)$$

### 3-4/ Synthesis method of HP-NGD circuits

The proposed synthesis method of HP-NGD circuit consists in calculating the components  $R$ ,  $R_m$  and  $L$  in function of the desired specifications. Doing this, we need three independent equations to realize the HP-NGD circuit synthesis.

#### 3-4-1/ Synthesis equations of the $R$ and $L$ parameters in function of the HP-NGD specifications

The inputs of the synthesis method calculation are the values of NGD specifications earlier indicated in Figs. 2 as:

- The NGD cut-off frequency:

$$\omega_n = 2\pi f_n \quad (29)$$

- The attenuation at the NGD cut-off frequency:

$$N_n = N(\omega_n) < 1 \quad (30)$$

- And the NGD:

$$GD_x = GD(\omega_x) < 0 \quad (31)$$

at the NGD optimal frequency.

The resistor,  $R_m$ , synthesis equation is obtained by inverting equation (18) which implies:

$$R_m = \frac{N_n^2 R}{1 - N_n^2}. \quad (32)$$

In addition, the inductor synthesis equation obtained from the cut-off frequency formulated in equation (17) is given by to the following equation:

$$L = \frac{R\sqrt{R_m}}{2\pi f_n \sqrt{R_m + R}}. \quad (33)$$

Substituting this expression of resistor,  $R_m$ , into the cut-off frequency formulated in equation (17), the inductor equation becomes:

$$L = \frac{N_n R}{2\pi f_n}. \quad (34)$$

Therefore, substituting equation (32) and equation (34) into equation (19), it yields the following optimal GD equation:

$$GD_x = \frac{(1-x^2)N_n R}{2\pi f_n \left[1 - N_n^2 + N_n^2(1+x^2)\right] \left[x^2(1-N_n^2) + N_n^2(1+x^2)\right]}. \quad (35)$$

By inverting this last equation, the synthesis equation of resistor can be expressed as:

$$R = \frac{2\pi f_n GD_x \left[1 - N_n^2 + N_n^2(1+x^2)\right] \left[x^2(1-N_n^2) + N_n^2(1+x^2)\right]}{(1-x^2)N_n R}. \quad (36)$$

These synthesis formulae enable to elaborate some analytical characteristics of the circuit topology under study.

### 3-4-2/ Characterization of HP-NGD circuit attenuation at the optimal frequency

The characterization aims to study the relation between the different attenuations and the ratio of the NGD optimal and cut-off frequency. The characteristic of the HP-NGD can be established in function of the chosen cut-off frequency,  $f_n$ , attenuation,  $N_n$ , and the optimal GD,  $GD_x$ . It is worth to note that the optimal attenuation,  $N_x$ , given by equation (21) can be expressed in function of the cut-off frequency attenuation,  $N_n$ , by the relationship:

$$N_x = \frac{N_n \sqrt{R + (1+x^2)R_m}}{\sqrt{x^2 R + (1+x^2)R_m}}. \quad (37)$$

The substitution of the resistor equation (32) and equation (36) into the previous expression implies systematically this modified optimal attenuation:

$$N_x = \frac{N_n \sqrt{1 - N_n^2 + N_n^2(1+x^2)}}{\sqrt{x^2(1-N_n^2) + N_n^2(1+x^2)}}. \quad (38)$$

The numerical calculations of this optimal attenuation in function of  $N_n$  varied from -10 dB to -1 dB and the ratio  $x$  varied from 1.1 to 10 gives the mapping displayed by Fig. 4(a). This 2-D cartographical mapping is practically useful to predict the optimal attenuation in function of the chosen parameters  $N_n$  and  $x$  during the HP-NGD circuit synthesis. It can be understood from this cartography that  $N_x$  increases with  $N_n$ . However, as illustrated by the three curves for  $N_n = \{-1 \text{ dB}, -2 \text{ dB}, -3 \text{ dB}\}$  shown in Fig. 4(b), the optimal attenuation is inversely proportional with the ratio  $x$ .

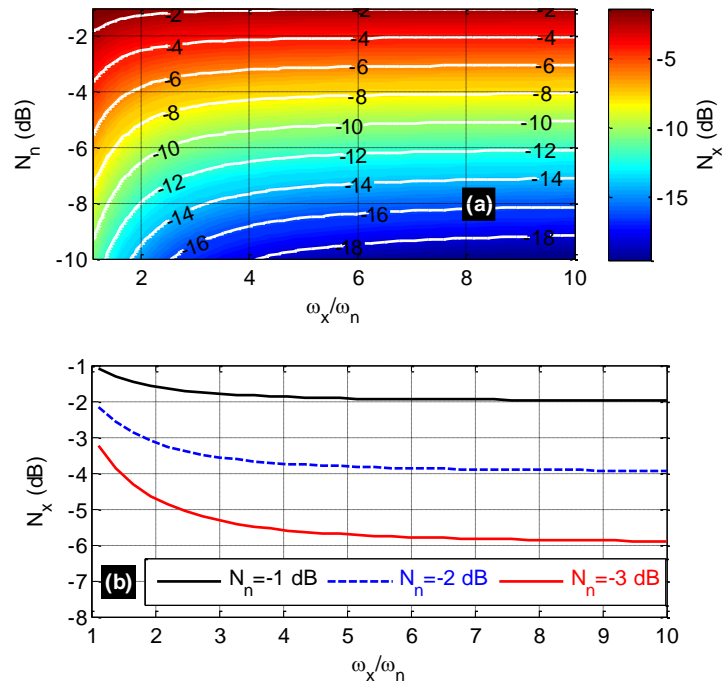


**Fig. 4: (a) 2-D mapping and (b) 1-D plot of the optimal attenuation versus the NGD optimal- and cut-off frequency ratio.**

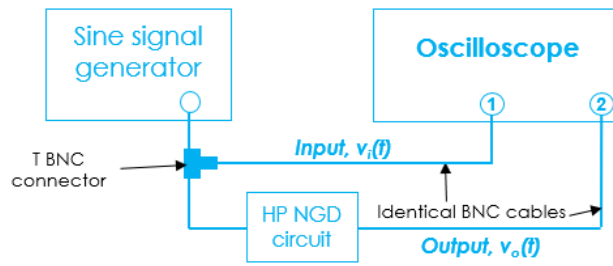
To validate the developed HP-NGD circuit theory, an experimental demonstrator will be discussed in the next section.

#### 4/ EXPERIMENTAL TEST DESCRIPTION

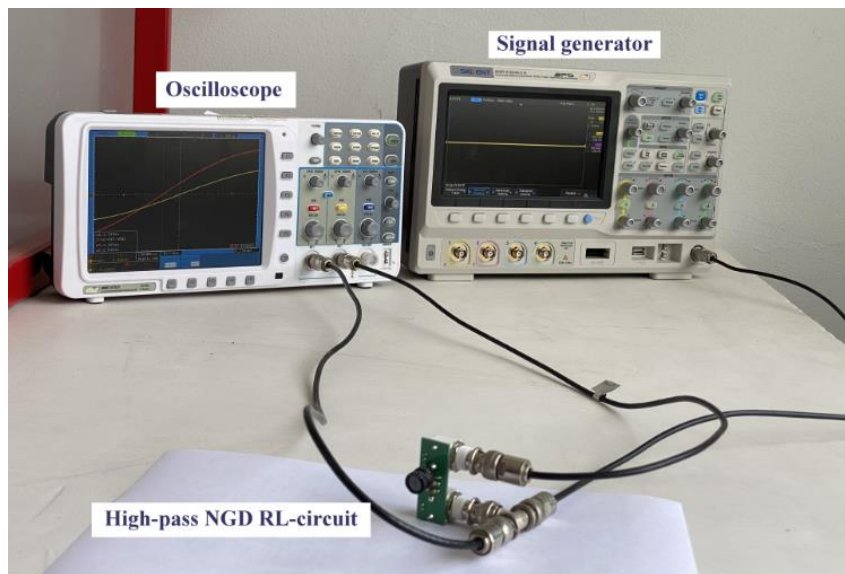
The present section describes the experimental validation of the HP-NGD theory of RL-network. After the POC description, the validation results will be discussed.

##### 4-1/ Experimentation technique

Fig. 5(a) highlights the experimental setup diagram of the BP NGD POC. The LF signal generator, referenced AKIP 4126/4A, generates a periodic sine signal at the input of the circuit. The input and the output signals are observed on oscilloscope referenced AKIP 4122/3. The RL-network circuit is mounted on fabricated as printed circuit board. The LF signal generator and the oscilloscope are connected to the circuit under test (CUT) via BNC cables as illustrated in Fig. 5(b). Table 1 summarizes the main specifications of the equipment's employed of the experimented HP-NGD circuits.



(a)



(b)

**Fig. 5: (a) Illustrative diagram and (b) photograph of the HP NGD circuit experimental setup.**

Description	References	Parameter	Value
Arbitrary function generator option	AKIP 4126/4A-X	Sampling rate	125 MS/s
		Bandwidth	25 MHz
Digital oscilloscope	AKIP 4122/3	Sampling rate	2 GS/s
		Bandwidth	100 MHz

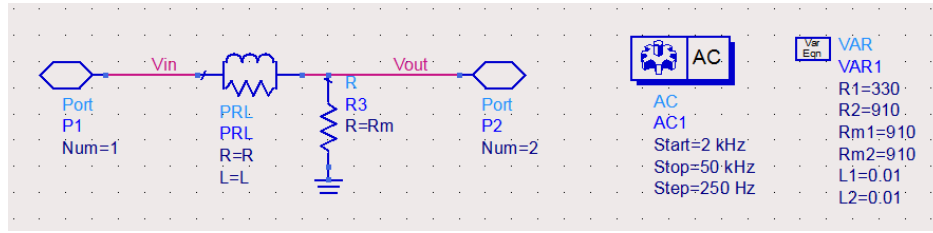
**Table 1: Specifications of the test equipment's**

The following subsection discusses and examines the results from the simulated, fabricated and tested HP-NGD circuit prototypes.

#### 4-2/ Fabricated HP-NGD circuit prototypes

Fig. 6(a) represents the schematic of simulated HP-NGD circuit from the ADS® environment. This simulation panel contains the circuit design, the component values of the two POCs and also the type of considered AC simulation. The photographs of the tested HP-NGD circuit prototypes are displayed by Fig. 6(b) and Fig. 6(c). After the consideration of the HP-NGD specifications, the ideal values of the simulated circuit are calculated. Table 2 addresses the references of the components constituting the two HP-NGD circuit prototypes. Then, the

nominal values of the used components which have 5% relative tolerances are indicated in the right side of Table 2.



(a)



(b)



(c)

**Fig. 6: (a) Schematic and (b)-(c) photographs of prototypes of tested HP NGD circuits.**

Description	References	Parameters	Nominal value
NGD circuit <sub>1</sub>	Resistor	$R_1$	330 $\Omega$
		$R_{m1}$	910 $\Omega$
	Inductor	$L_1$	10 mH
NGD circuit <sub>2</sub>	Resistor	$R_2$	910 $\Omega$
		$R_{m2}$	910 $\Omega$
	Inductor	$L_2$	10 mH

**Table 2: Component values and references**

With the fabricated HP-NGD circuit prototype, the formulation method of the NGD responses are indicated in the following subsection.

#### 4-3/ Formulation of measured HP-NGD responses

The HP-NGD responses from the experimental setup introduced in the previous subsection are obtained from the input and output sine responses. The  $t$ -time dependent input sine signal can be expressed in function of the test frequency,  $f_k$  and amplitude,  $A_{max}$ , by the equation:

$$v_{in}(t) = A_{max} \sin(2\pi f_k t). \quad (39)$$

Acting as a linear time-invariant, the associated output signal can be expressed by:

$$v_{out}(t) = B_{max} \sin(2\pi f_k t + \Delta\varphi). \quad (40)$$

The HP-NGD circuit measurement consists originally in sweeping the frequency  $f_k$  of the input sine signal from  $f_{min}=1$  kHz to  $f_{max}=50$  kHz. During the test, we choose the frequency step equal to  $\Delta f=50$  Hz. The input signal was windowed over the time width of  $\Delta t=40$   $\mu$ s. We recorded during the tests the amplitudes and phases of the input and output sine signals. Then, the measured amplitudes and phase shift of the measured circuit VTF were calculated from the classical equations:

$$T_{measured}(f_k) = \frac{B_{max}(f_k)}{A_{max}(f_k)} \quad (41)$$

$$\varphi_{measured}(f_k) = \Delta\varphi(f_k). \quad (42)$$

Accordingly, the GD response is determined by:

$$GD_{measured}(f_k) = \frac{\varphi_{measured}(f_k) - \varphi_{measured}(f_{k-1})}{2\pi(f_k - f_{k-1})} \quad (43)$$

where the integer  $k$  varies from 2 to  $k_{max}$ .  $A_{max}$  and  $B_{max}$  are the input and output signal amplitudes:

$$k_{max} = Ent \left[ \frac{f_{max} - f_{min}}{\Delta f} \right]. \quad (44)$$

In this equation, the quantity,  $Ent[x]$  presents the superior integer part of real  $x$ . By using the developed HP-NGD circuit measurement techniques, we obtained the results explored in the following section.

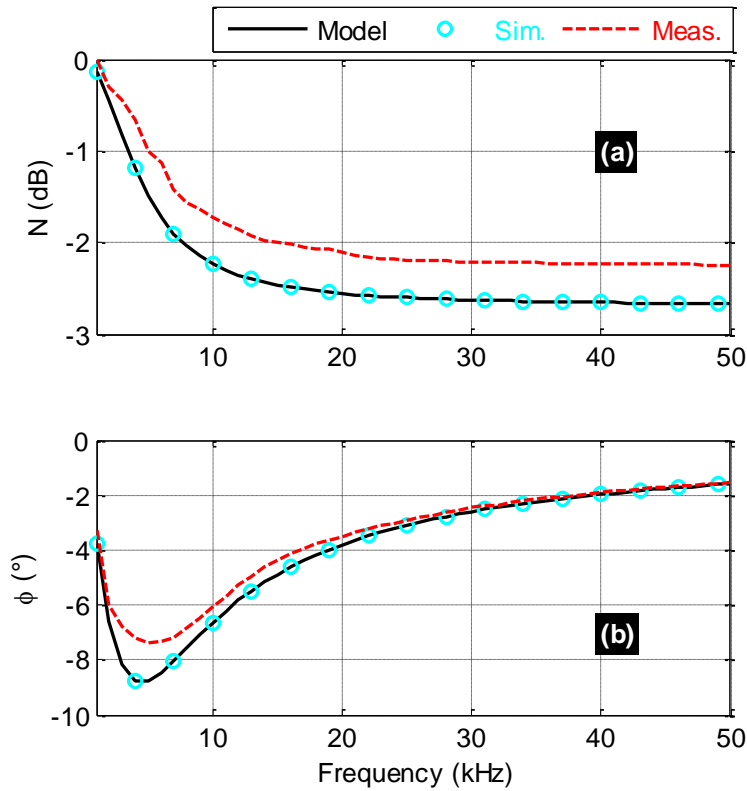
## 5/ HP-NGD FUNCTION VALIDATION RESULTS

This section introduces the discussion on the simulated and measured validation results of the POCs HP-NGD circuits introduced previously. The results of the two HP-NGD circuit prototypes will be investigated in the following subsections.

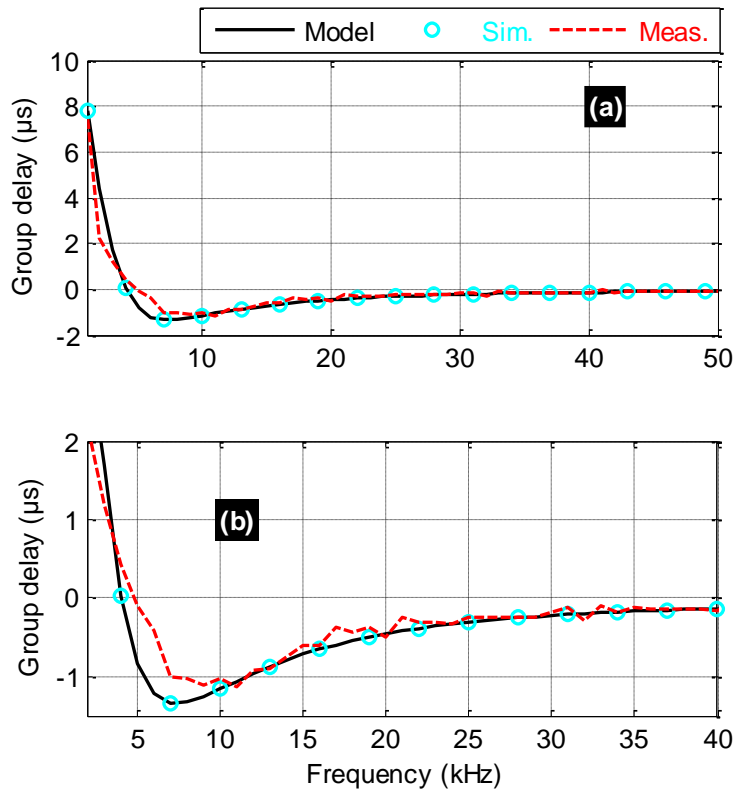
### 5-1/ Discussion on the results of HP-NGD circuit prototype<sub>1</sub>

Fig. 7(a) and Fig. 7(b) represent the VTF magnitudes and phases of the calculated model (“Model”, black solid line), simulated results (“Sim.”, blue dotted line) and measured results (“Meas.”, red dashed line) of tested circuit prototype<sub>1</sub>. The associated wide band and zoomed in narrow band GDs are displayed by Figs. 8. It can be pointed out that the results of calculation, simulation and measurement are particularly in good correlation. We can underline that the GD response confirm the HP-NGD function of the tested RL-circuit. The GDs are positive at VLFs and become negative above the cut-off frequencies. Table 3 indicates the comparisons of the HP-NGD circuit specifications. We can see that the NGD cut-off frequency is of about 4 MHz according to the calculation and simulation against 5 MHz according to the measurement result. The slight difference of the measured magnitude about 0.5 dB is essentially due to:

- The lumped component tolerances of the RL-network circuit prototype<sub>1</sub>,
- The imperfections of the PCB fabrications,
- And the systematic errors from the measurement techniques induced by the oscilloscopes and the used cable-connect networks.



**Fig. 7:** Calculated, simulated and measured (a) magnitude and (b) phase responses of tested HP-NGD prototype<sub>1</sub> with  $R_1=330 \Omega$ ,  $R_{m1}=910 \Omega$  and  $L_1=10$  mH.



**Fig. 8:** Calculated, simulated and measured (a) wide-band and (b) narrow-band GD responses of tested HP-NGD prototype<sub>1</sub> with  $R_1=330 \Omega$ ,  $R_{m1}=910 \Omega$  and  $L_1=10$  mH.

Parameters	Name	Model	Simulation	Measurement
Cut-off frequency	$f_n$	4 MHz	4 MHz	5 MHz
Attenuation	$T(f_n)$	-1.19 dB	-1.19 dB	-1 dB
Optimal frequency	$f_x$	7.5 MHz	7.52 MHz	9 MHz
Optimal GD	$GD_x$	-1.33 $\mu$ s	-1.34 $\mu$ s	-1.12 $\mu$ s
Optimal attenuation	$T(f_x)$	-2.01 dB	-2.01 dB	-1.64 dB

**Table 3: HP-NGD specifications of prototype<sub>1</sub>**

#### 4-2/ Discussion on the results of HP-NGD circuit prototype<sub>2</sub>

The present paragraph examines the validation results of the tested circuit prototype<sub>2</sub>. The results are similar to the previous case of prototype<sub>1</sub>. The HP-NGD function is validated by the behavior of the calculated, simulated and measured GD responses. Fig. 9(a) and Fig. 9(b) show the VTF magnitudes and phases of the calculated model, simulated results and measured results which are indicated by legends “Model” (black solid line), simulated “Sim.” (blue dotted line) and “Meas.” (red dashed line). Figs. 10 depict the associated GD responses. When we follow the curves following the increase of frequency, we can see that the plots of the modeled, simulated and measured GD start from positive value and becomes negative above the NGD cut-off frequency.

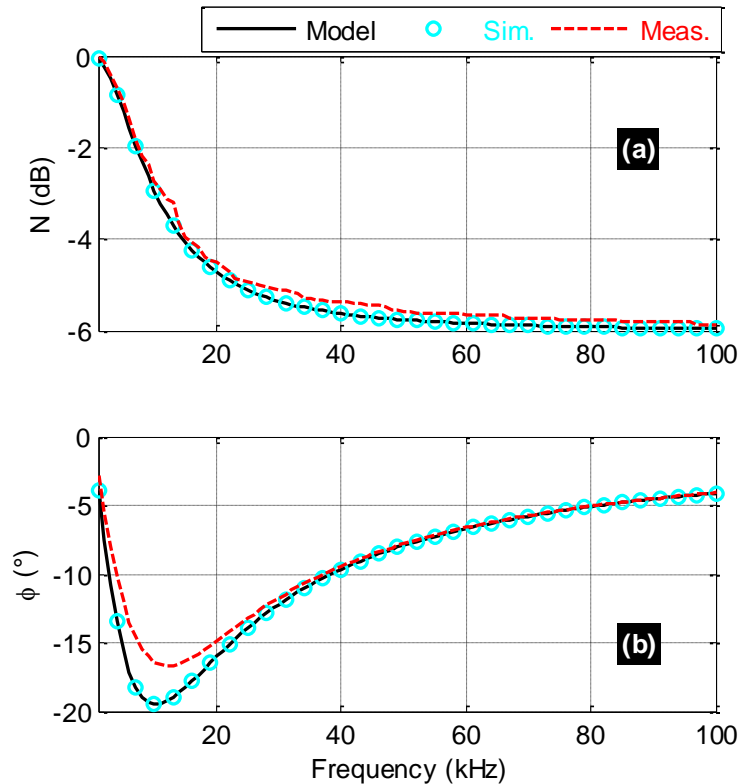


**Fig. 9: Calculated, simulated and measured (a) magnitude and (b) phase responses of tested HP-NGD prototype<sub>2</sub> with  $R_2=910 \Omega$ ,  $R_{m2}=910 \Omega$  and  $L_2=10$  mH.**

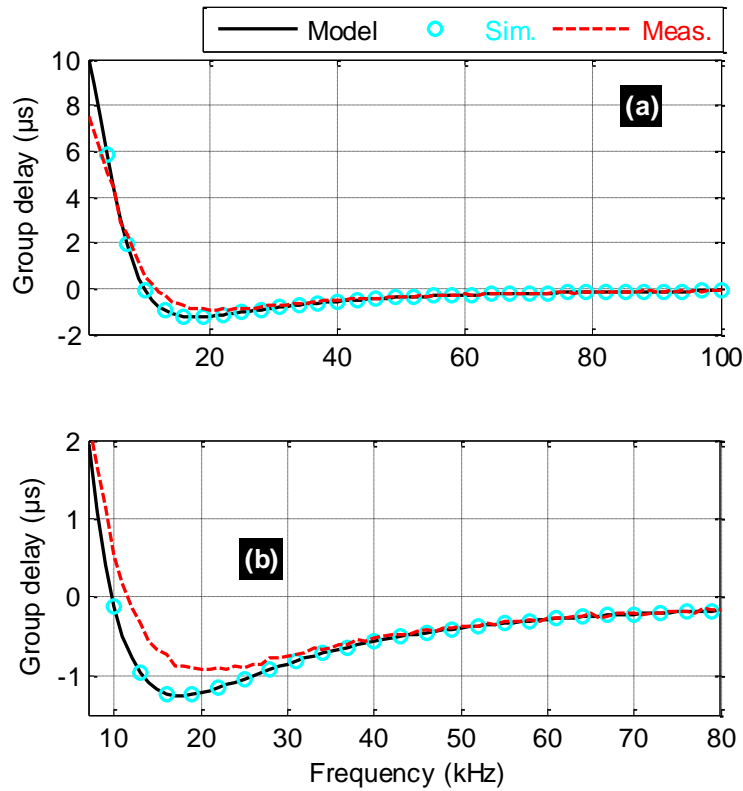


**Fig. 10: Calculated, simulated and measured (a) wide-band and (b) narrow-band GD responses of tested HP-NGD prototype<sub>2</sub> with  $R_2=910 \Omega$ ,  $R_{m2}=910 \Omega$  and  $L_2=10 \text{ mH}$ .**

Parameters	Name	Model	Simulation	Measurement
Cut-off frequency	$f_n$	9.78 MHz	9.801 MHz	11.7 MHz
Attenuation	$T(f_n)$	-2.9 dB	-2.94 dB	-2.99 dB
Optimal frequency	$f_x$	17 MHz	17.02 MHz	21 MHz
Optimal GD	$GD_x$	-1.25 $\mu\text{s}$	-1.25 $\mu\text{s}$	-0.92 $\mu\text{s}$
Optimal attenuation	$T(f_x)$	-4.37 dB	-4.37 dB	-4.81 dB

**Table 4: HP-NGD specifications of prototype<sub>2</sub>**

Such results correspond clearly to the behavior of HP-NGD function. Table 4 gives the comparative values of the calculated, simulated and measured specifications around the NGD cut-off and optimal frequencies. The differences between the experimental results and the other ones are caused by the same reasons as the previous case of study.

## 5/ CONCLUSION

A particular innovative study of unfamiliar lumped passive circuit is investigated. The study is using an RL-network based HP-NGD topology.

The basic specifications of the HP-NGD function are defined. The circuit analytical investigation is elaborated from the VTF expression. The detailed expressions of the NGD cut-off frequency and the optimal NGD value are

established. In addition, a particular original formulation of the HP-NGD topology attenuation at the cut-off and optimal frequencies are theoretically expressed in function of the R and L parameters. The synthesis equations enabling to determine these parameters in function of the desired HP-NGD specifications are expressed. In addition, the characterization of the attenuation is proposed.

The HP-NGD theory is validated by the feasibility study based on the design and fabrication of the POC prototype of PCBs. As expected, the calculated, simulated and measured magnitudes and GDs are good agreement. More importantly, the three validation results confirm the HP-NGD behavior of the frequency responses of the tested PCBs.

## 6/ REFERENCES

- [1] G. Groenewold, "Noise and Group Delay in Active Filters," *IEEE Trans. CAS I: Regular Papers*, Vol. 54, No. 7, July 2007, pp. 1471-1480.
- [2] S.-S. Myoung, B.-S. Kwon, Y.-H. Kim and J.-G. Yook, "Effect of Group Delay in RF BPF on Impulse Radio Systems," *IEICE Tran. Communications*, Vol. 90, No. 12, 2007, pp. 3514-3522.
- [3] S.-M. Kang and H. Y. Chen, "A global delay model for domino cmos circuits with application to transistor sizing," *I. J. Circuit Theory and Applications*, vol. 18, no. 3, pp. 289-306, May/June 1990.
- [4] B. Ravelo, "Delay Modelling of High-Speed Distributed Interconnect for the Signal Integrity Prediction," *Eur. Phys. J. Appl. Phys.*, Vol. 57 (31002), Feb. 2012, pp. 1-8.
- [5] N. S. Bukhman, "On the distortion of the rising edge of a carrier-free signal," *J. Commun. Technol. Electron.* 61, 1327–1337 (2016).
- [6] N. S. Bukhman, "On the Distortion of the Leading Edge of a Quasi-Monochromatic Signal in a Resonantly Absorbing Medium," *J. Commun. Technol. Electron.* 64, 203–216 (2019).
- [7] H. F. Li, S. C. Leung and P. N. Lam, "Optimised Synthesis of Delay-Insensitive Circuits Using Time-Sharing," *IEE Proceedings - Computers and Digital Techniques*, Vol. 141, No. 2, Mar. 1994, pp. 111-118.
- [8] S. V. Narasimhan, M. Hazarathiah and P. V. S. Giridhar, "Channel Blind Identification Based on Cyclostationarity and Group Delay," *Signal Processing*, Vol. 85, No. 7, July 2005, pp. 1275-1286.
- [9] E. C. Heyde, "Theoretical Methodology for Describing Active and Passive Recirculating Delay Line Systems," *Electronics Letters*, Vol. 31, No. 23, Nov. 1995, pp. 2038-2039.
- [10] J. Vemagiri, A. Chamarti, M. Agarwal and K. Varahramyan, "Transmission Line Delay-Based Radio Frequency Identification (RFID) Tag," *Microwave and Optical Technology Letters*, Vol. 49, No. 8, Aug. 2007, pp. 1900-1904.
- [11] L. N. Alves and R. L. Aguiar, "A time-delay technique to improve GBW on negative feedback amplifiers," *International Journal of Circuit Theory and Applications*, Vol. 36, No. 4, June 2008, pp. 375-386.
- [12] B. Ravelo, S. Lall ch re, A. Thakur, A. Saini and P. Thakur, "Theory and circuit modelling of baseband and modulated signal delay compensations with low- and band-pass NGD effects," *Int. J. Electron. Commun.*, Vol. 70, No. 9, Sept. 2016, pp. 1122–1127.

- [13] T. Shao, Z. Wang, S. Fang, H. Liu and Z. N. Chen, "A group-delay-compensation admittance inverter for full-passband self-equalization of linear-phase band-pass filter," *Int. J. Electron. Commun.*, Vol. 123, No. 153297, 2020, pp. 1-6.
- [14] T. Zhang, R. Xu and C. M. Wu, "Unconditionally Stable Non-Foster Element Using Active Transversal-Filter-Based Negative Group Delay Circuit," *IEEE Microw. Wireless Compon. Lett.*, vol. 27, no. 10, pp. 921-923, Oct. 2017.
- [15] B. Ségard and B. Macke, "Observation of Negative Velocity Pulse Propagation," *Phys. Lett. A*, Vol. 109, 1985, pp. 213-216.
- [16] B. Macke and B. Ségard, "Propagation of light-pulses at a negative group-velocity," *Eur. Phys. J. D*, Vol. 23, 2003, pp. 125–141.
- [17] N. S. Bukhman, "On the Principle of Causality and Superluminal Signal Propagation Velocities," *Journal of Communications Technology and Electronics*, vol. 66, pp. 227–241, Apr. 2021.
- [18] N. S. Bukhman, "On the propagation velocity of a wave packet in an amplifying medium," *Quantum Electronics*, vol. 31, no. 9, pp. 774-780, 2001.
- [19] N. S. Bukhman, "On the reality of supraluminal group velocity and negative delay time for a wave packet in a dispersion medium," *Tech. Phys.*, vol. 47, pp. 132-134, (2002).
- [20] A. Dogariu, A. Kuzmich, and L. J. Wang, "Transparent anomalous dispersion and superluminal light-pulse propagation at a negative group velocity," *Phys. Rev. A* 63, 053806, pp. 1-12, Apr. 2001.
- [21] G. V. Eleftheriades, O. Siddiqui, and A. K. Iyer, "Transmission Line for Negative Refractive Index Media and Associated Implementations without Excess Resonators," *IEEE Microw. Wireless Compon. Lett.*, Vol. 13, No. 2, pp. 51-53, Feb. 2003.
- [22] O. F. Siddiqui, M. Mojahedi and G. V. Eleftheriades, "Periodically Loaded Transmission Line With Effective Negative Refractive Index and Negative Group Velocity," *IEEE Trans. Antennas Propagat.*, Vol. 51, No. 10, Oct. 2003, pp. 2619-2625.
- [23] L. Markley and G. V. Eleftheriades, "Quad-Band Negative-Refractive-Index Transmission-Line Unit Cell with Reduced Group Delay," *Electronics Letters*, Vol. 46, No. 17, Aug. 2010, pp. 1206-1208.
- [24] G. Monti and L. Tarricone, "Negative Group Velocity in a Split Ring Resonator-Coupled Microstrip Line," *Progress In Electromagnetics Research*, Vol. 94, pp. 33-47, 2009.
- [25] N. S. Bukhman and S. V. Bukhman, "On the Negative Delay Time of a Narrow-Band Signal as It Passes through the Resonant Filter of Absorption," *Radiophysics and Quantum Electronics*, Vol. 47, No. 1, 2004, pp. 66-76.
- [26] M. W. Mitchell, and R. Y. Chiao, "Negative group delay and "fronts" in a causal system: An experiment with very low frequency bandpass amplifiers," *Phys. Lett. A*, vol. 230, no. 3-4, June 1997, pp. 133-138.
- [27] M. W. Mitchell and R.Y. Chiao, "Causality and Negative Group-delays in a Simple Bandpass Amplifier," *Am. J. Phys.*, vol. 66, 1998, pp. 14-19.
- [28] T. Nakanishi, K. Sugiyama and M. Kitano, "Demonstration of Negative Group-delays in a Simple Electronic Circuit," *Am. J. Phys.*, vol. 70, no. 11, 2002, pp. 1117-1121.
- [29] M. Kitano, T. Nakanishi and K. Sugiyama, "Negative Group-delay and Superluminal Propagation: An Electronic Circuit Approach," *IEEE J. Sel. Top. in Quantum Electron.*, vol. 9, no. 1, Feb. 2003, pp. 43-51.

- [30] J. N. Munday and R. H. Henderson, "Superluminal Time Advance of a Complex Audio Signal," *Appl. Phys. Lett.*, vol. 85, no. 3, July 2004, pp. 503-504.
- [31] H. Mao, L. Ye and L.-G. Wang, "High fidelity of electric pulses in normal and anomalous cascaded electronic circuit systems," *Results in Physics*, vol. 13, no. 102348, pp. 1-9, June 2019.
- [32] M. Kandic and G. E. Bridges, "Bilateral Gain-Compensated Negative Group Delay Circuit," *IEEE Microwave and Wireless Components Letters*, Vol. 21, No. 6, May 2011, pp. 308-310.
- [33] M. T. Abuelma'atti and Z. J. Khalifa, "A new CFOA-based negative group delay cascadable circuit," *Analog Integrated Circuits and Signal Processing*, vol. 95, pp. 351-355, Mar. 2018.
- [34] Y. Meng, Z. Wang, S. Fang, T. Shao and H. Liu, "A Broadband Switch-Less Bi-Directional Amplifier with Negative-Group-Delay Matching Circuits," *Electronics*, vol. 7, no. 9, (158), 2018, pp. 1-11.
- [35] B. Ravelo, "Similitude between the NGD function and filter gain behaviours," *Int. J. Circ. Theor. Appl.*, Vol. 42, No. 10, Oct. 2014, pp. 1016–1032.
- [36] B. Ravelo, "On low-pass, high-pass, bandpass, and stop-band NGD RF passive circuits," in *URSI Radio Science Bulletin*, vol. 2017, no. 363, pp. 10-27, Dec. 2017.
- [37] B. Ravelo, "First-order low-pass negative group delay passive topology," *Electronics Letters*, Vol. 52, No. 2, Jan. 2016, pp. 124–126.
- [38] B. Ravelo, "High-Pass Negative Group Delay RC-Network Impedance," *IEEE Transactions on Circuits and Systems II: Express Briefs*, Vol. 64, No. 9, Sept. 2017, pp. 1052-1056.